

Adversarial Attacks on Deep Learning-based Video Compression and Classification Systems

Jung-Woo Chang¹, Mojan Javaheripi¹, Seira Hidano², Farinaz Koushanfar¹

¹University of California San Diego

²KDDI Research, Inc.

Abstract

Video compression plays a crucial role in enabling video streaming and classification systems and maximizing the end-user quality of experience (QoE) at a given bandwidth budget. In this paper, we conduct the first systematic study for adversarial attacks on deep learning based video compression and downstream classification systems. We propose an adaptive adversarial attack that can manipulate the Rate-Distortion (R - D) relationship of a video compression model to achieve two adversarial goals: (1) increasing the network bandwidth or (2) degrading the video quality for end-users. We further devise novel objectives for targeted and untargeted attacks to a downstream video classification service. Finally, we design an input-invariant perturbation that universally disrupts video compression and classification systems in real time. Unlike previously proposed attacks on video classification, our adversarial perturbations are the first to withstand compression. We empirically show the resilience of our attacks against various defenses, i.e., adversarial training, video denoising, and JPEG compression. Our extensive experimental results on various video datasets demonstrate the effectiveness of our attacks. Our *video quality* and *bandwidth attacks* deteriorate peak signal-to-noise ratio by up to 5.4dB and the bit-rate by up to $\sim 2.4\times$ on the standard video compression datasets while achieving over 90% attack success rate on a downstream classifier.

1 Introduction

Video content accounts for more than 80% of the internet traffic [45]. Live video traffic has experienced an even higher growth with the advent of streaming services, e.g., YouTube Live [2] and Twitch.tv [1]. In addition, recent developments in deep learning have given rise to live video analysis services such as activity recognition for health care diagnosis [16], video surveillance [44], and autonomous vehicles [20]. Video compression technologies are a key enabler for the aforesaid media streaming and content analysis applications.

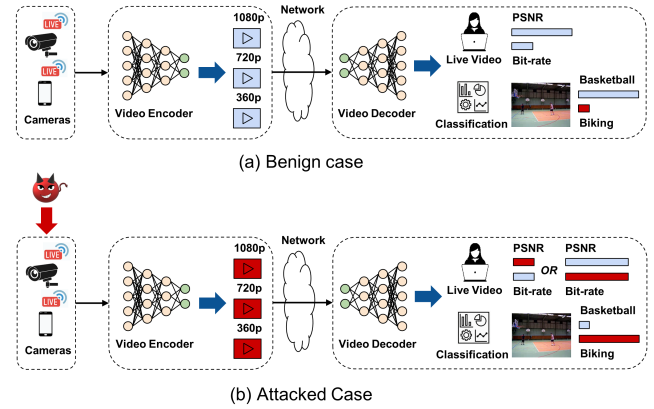


Figure 1: (a) High-level view of a live video streaming and classification system. (b) High-level overview of our proposed attack, performed by injecting adversarial perturbations to the cameras. To demonstrate the adversarial effect, we present the peak signal-to-noise ratio (PSNR), bit-rate, and an example outcome of video activity recognition.

As shown in Figure 1-(a), live video streaming and classification systems typically consist of four main components, i.e., front-end video sources (cameras), video encoder, video decoder, and back-end video subscribers. In this setting, the video encoder and decoder compress the video for efficient real-time streaming to back-end subscribers. Recent literature proposes Deep Neural Network (DNN) based encoder and decoders for video compression [17, 31, 55]. Due to their enhanced performance over conventional hand-crafted codecs [43, 51], DNNs are now leveraged to develop the next generation of video compression technologies.

Signal transformation techniques, e.g., compression, have been trusted to remove the adversarial effect in image recognition [3, 19, 29, 36]. We empirically show that the state-of-the-art adversarial instances created for video classification [24, 25, 50] can also be eliminated after passing through the video compression pipeline. Nevertheless, the robustness of the DNN-based video compression pipeline itself against adversarial perturbations remains largely unknown to date.

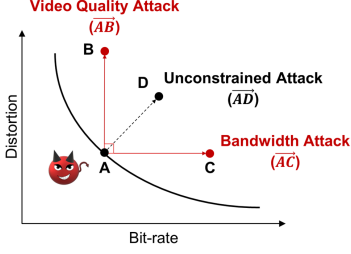


Figure 2: Effect of adversarial attacks on the R - D curve shown for: video quality attack (\overrightarrow{AB}), bandwidth attack (\overrightarrow{AC}), and an unconstrained attack (\overrightarrow{AD}).

We show, for the first time, that DNN-based video compression systems can be exploited by adversaries to not only reduce the users’ quality of experience (QoE), but also attack downstream video recognition services. The success of our attacks is indebted to solving a novel unified optimization problem. The solution crafts adversarial perturbations that simultaneously attack the video compression and the downstream video classification system as shown in Figure 1-(b).

Proposed Attacks. The goal of video compression is to simultaneously minimize the number of bits used for encoding while reducing the distortion. Contemporary DNN-based video compression frameworks [17, 31, 55] typically employ a rate-distortion (R - D) optimization that minimizes a cost function trading off bit-rate (R) and distortion (D). In this paper, we aim to break the R - D model of a pre-trained video compression model. As shown in Figure 2, our attack objective is to rapidly increase R (or D) depending on the target scenario, while maintaining the other metric. Note that when R and D both change, the streamer can easily notice the attack by looking at the R - D curve as illustrated in Figure 2.

We propose two novel QoE attacks on video compression: a *video quality attack* and a *bandwidth attack*. The video quality attack increases D while keeping R constant, whereas the bandwidth attack reduces the compression rate by increasing R while maintaining D . We also propose a *compression-robust classifier attack* that causes misclassification of all the actions in the video by a downstream video recognition service. Notably, this is the first attack on video classification that remains successful even if the perturbed video goes through various signal transformations, i.e., video compression, video denoising, and frame-by-frame JPEG compression.

Our attacks are applicable to both online and offline settings. In the offline scenario, videos are locally stored in a camera or smartphone and the attacker does not have a latency constraint. For the challenging online scenario, we preprocess universal perturbations that can attack any video stream in real time. We assume a white-box threat model when constructing our attacks since video compression models are publicly available and their architecture and parameters are standard.

Design Challenges and Solutions. We are faced with several new design challenges not present in prior work that attack only video classification [24, 25, 35, 50, 52]. Firstly,

video compression systems, by design, are extremely robust to noise. State-of-the-art video coding schemes [17, 31, 55] group a series of frames into sequences called Group of Pictures (GOP) to allow back-end users to access live video streams at any time. The GOP structure inherently improves robustness against error propagation and sudden scene changes during compression, thereby making the adversarial attack more challenging. We address this problem by averaging the distortion and bit-rate in individual GOPs, not the entire video as commonly used in video classification attacks. By leveraging the independence between GOPs in the training of adversarial noise, we achieve perturbations that are robust to compression. We systematically validate the effectiveness of our proposed attacks on two types of widely used GOP structures [31, 55].

Secondly, previous attacks [24, 25, 35, 50, 52] on video recognition do not consider video compression in their threat models. Recent work shows that conventional compression algorithms can be used as a defense against adversarial attacks to classification [3, 19, 29, 36]. Specifically, lossy compression with quantization reduces the spatiotemporal data, thereby easily removing the adversarial perturbations. To provide a compression-resistant perturbation for video recognition, we consider the video compression in our adversarial attack. In the video compression pipeline, the reconstruction error is propagated to the next frame during encoding. Consequently, we design a new model to train the perturbations by using the information from different time steps and combining all information to break the original R - D optimization.

Finally, the adversary does not have prior knowledge about the content of the streaming video. While launching the online attacks, the perturbation should be effectively injected at any time in the video. Specifically, the perturbations should be well aligned with the streamed video frames or otherwise will lose their effect [25, 52]. To tackle this challenge, we utilize a temporal transformation function during the training process. This enables us to learn a universal adversarial perturbation that can perform the attack in any order of the video sequence. In summary, our key contributions are as follows:

- We perform the first systematic study on adversarial attacks to deep learning based video compression systems. We further exploit the video compression to direct our attacks towards downstream video recognition systems.
- We propose three new adversarial attacks that result in high-impact security and QoE consequences. We formalize our attacks as well-defined optimization problems that can be solved to obtain perturbations affecting the video quality, bandwidth, and downstream classification.
- We construct an input-invariant universal perturbation that can be injected at any time during live video streaming and classification. This enables us to conduct our attack in real time under strict latency constraints.
- Our adversarial attacks are the first of their kind to withstand the inherent denoising performed during video compression. Additionally, we show the resiliency of

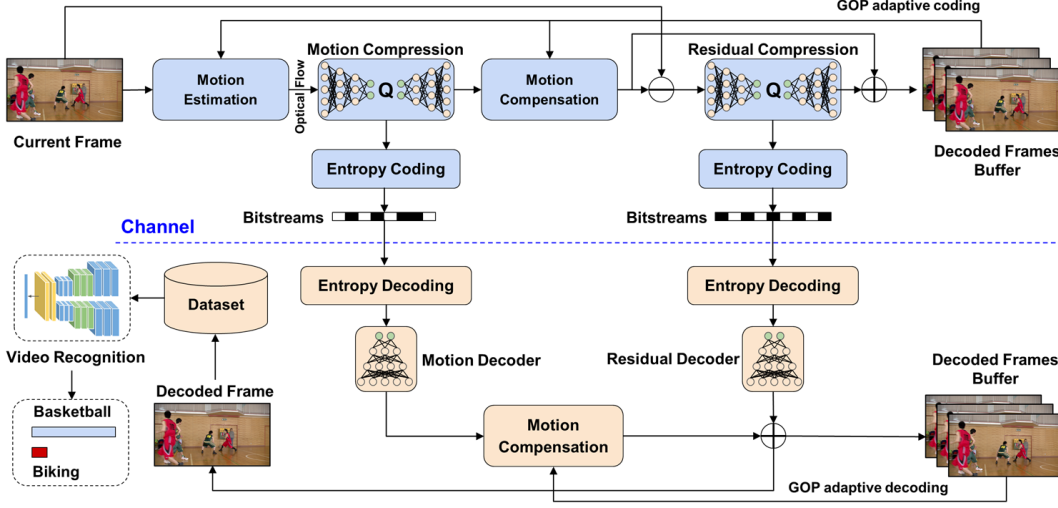


Figure 3: Overview of the DNN-based video compression and classification frameworks. Blue (resp. pink) color modules compose the video encoder (resp. decoder).

our attacks against various defenses namely, adversarial training, video denoising, and JPEG compression.

2 Preliminaries

Figure 3 illustrates an overview of the DNN-based video compression and classification framework. Video compression employs a temporal prediction structure to minimize the difference between the previously decoded frame and the current frame. The encoder sends bitstreams that conform to a specific channel standard to the decoder. The compressed video is then reconstructed from the bitstream by the decoder. We study two state-of-the-art video compression models, i.e., DVC [31] and HLVC [55] as our attack target.

We further include an optional video classifier as the target downstream task. This module predicts the activities performed in the video and is commonly deployed in video analysis services. As shown in Figure 3, the downstream video classification service receives as input the decoded frames from the video compression pipeline. We consider three state-of-the-art video classification models representing diverse methodologies, i.e., I3D [8], SlowFast [14], and TPN [54], as our victim models to attack. In what follows, we explain the internal mechanisms of the video compression modules shown in Figure 3. Throughout the paper, we use “video compression” and “video coding” interchangeably.

Temporal Coding Structure. Since back-end viewers can join the live video stream at random points, the bitstreams are transmitted in GOP units for error resiliency. We systematically analyze our attacks on two GOP structures widely used in video compression, namely, the non-hierarchical [31] and hierarchical coding prediction structure [55]. Specifically, DVC follows the non-hierarchical coding whereas HLVC

follows the hierarchical adaptive coding structure. Figure 4 shows a high-level view of the GOP structures in our paper.

A GOP contains different picture types, i.e., an I frame and several P and B frames. Within each GOP, the first frame, called I frame, is coded independently using image compression. We use a CNN-based image compression algorithm [28] to efficiently encode the I frame so that the P and B frames can refer to it with high quality. The P and B frames, which occupy most of the GOP, are constructed using video compression to remove temporal redundancy. Specifically, the P frame references the previous picture for motion estimation and compensation. The B frame uses both previous and forward frames for motion estimation and compensation to achieve the highest amount of compression.

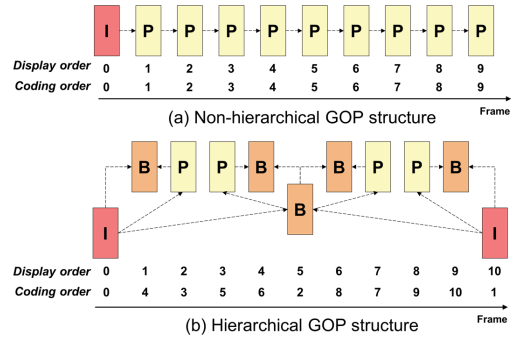


Figure 4: Non-hierarchical (top) and hierarchical (bottom) GOP structures for temporal prediction coding. Unlike non-hierarchical structure, the coding order of hierarchical structure is different from the display order.

Video Encoder. The encoder module uses a DNN-based motion estimation algorithm [37] to measure the movement be-

tween the current frame and the previous reconstructed frame, dubbed the optical flow map. Instead of directly quantizing the optical flow map, an auto-encoder network is employed to compress the pixel-wise motion difference with a high compression rate. The compressed optical flow map is then quantized using the motion compression method proposed in [5]. The encoder also includes a CNN-based pixel-wise motion compensation module. This module predicts the current frame using the reconstructed optical flow map and the previous frames. The residual frame is then computed using the current frame and the prediction. The residual amount is compressed using a non-linear residual encoder network that efficiently quantizes the redundancy in the latent space. Finally, the quantized latent representations from the motion compression and residual compression are converted to bitstreams via entropy coding [4] and sent to the decoder.

Video Decoder. After receiving the bitstreams from the video encoder, the decoder recovers the same quantized latent representations using entropy decoding. The decoder then applies motion and residual decoders to the latent representations and obtains the reconstructed optical flow map and residual frame. Similar to the encoder side, the decoder includes a motion compensation module that predicts the new frame using information from the previous frames and the reconstructed optical flow map. The predicted frame and the reconstructed residual frame are added to create the decoded frame, which is then stored in a buffer. The decoder is thus able to reconstruct each frame with a similar visual quality as the encoder.

3 Threat Model

3.1 Attack Scenarios

Our attacks are targeted towards video data generated by front-end sources (e.g., smartphones and surveillance cameras) that is sent to back-end user(s) through a video compression pipeline. Since prior work on adversarial video [35, 50, 52] do not consider the intervention of video compression, their perturbations are mostly eliminated as the video is compressed. As such the effect of previously proposed attacks on video classification will in fact not reach the target back-end user. To address this problem, our proposed attacks modify the video data at the first stage in the entire video compression and classification systems as shown in Figure 1-(b).

Our attacks are applicable to both *online* and *offline* scenarios. The online attack directly perturbs the front-end sources as the video is generated in real time. For this scenario, we design well-crafted universal perturbations that can be used to attack any given video sequence in real time. The offline attack adds perturbations to a temporarily stored video. Our offline scenario is analogous to the assumptions made in adversarial attacks on images [15, 40, 46] and audio signals [7, 26].

We note that video compression is not only used for live streaming, but also for various applications where the data

is archived in the cloud. In this context, the target video can be raw data in the original quality or compressed data. Even if the video has already been compressed, the adversary can restore the video with a decoder, inject a perturbation, and re-compress it. We consider the following two offline attack scenarios: 1) the adversary accesses the original raw data and perturbs the video, 2) the adversary decodes the compressed data, then inserts the compression-robust perturbation to the decoded video and re-encodes it. Through the above offline scenarios, the adversary can craft perturbed videos before the victim puts them in storage.

3.2 Adversary’s Goal

Throughout this paper, we use the terms “attacker” and “adversary” interchangeably. The adversary’s goal is to selectively degrade the bitrate R or distortion level D compare to a pre-trained R - D curve for the video encoder and decoder. We also optionally target our attacks towards a downstream video recognition model, causing misclassification of the decoded videos. We introduce the following three novel attacks:

Video Quality Attack. We formulate this attack to increase the distortion D at a given bit-rate. This, in turn, adds unwanted noise to the video content and reduces the visual quality for the viewers. This attack scenario is particularly advantageous when the media server administrator is monitoring the network bandwidth in real time. In this situation, the service provider can detect anomalies in the bit-rate, but the proposed distortion attack remains stealthy.

Bandwidth Attack. Our proposed bandwidth attack is formulated to increase R at a given distortion level. This, in turn, lowers the compression rate of the video encoder and subsequently increases the amount of data transfer on the underlying network channel. Due to the increased traffic, the video transcoder lowers the video’s resolution to match the acceptable channel bandwidth [22]. Thus, by targeting R as the attack objective, the adversary can reduce the resolution of videos viewed by back-end users.

Compression-robust Classifier Attack. Our final attack manipulates the classification result of the decoded video in scenarios where the downstream task uses a deep-learning based video recognition system. This attack is particularly challenging as the video compression framework inherently invalidates most adversarial examples using CNN-based temporal prediction coding schemes and quantization. As such, we carefully craft an optimization problem that enables us to generate adversarial perturbations that are robust to video compression. We propose two variants of the classifier attack, namely, targeted and untargeted [50], depending on the adversary’s goal. Targeted attacks misguide the video classifier to a particular class while untargeted attacks subvert the models to predict any of the incorrect classes.

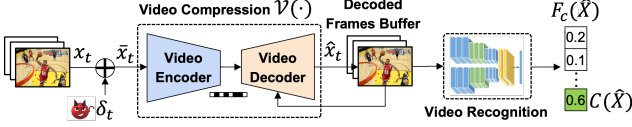


Figure 5: Overview of system components for the proposed adversarial attack to video compression and classification.

3.3 Adversary’s Capability and Knowledge

Video coding standards are jointly determined by various standardization organizations, e.g., the ISO/IEC Moving Picture Experts Group (MPEG), ITU-T Video Coding Experts Group (VCEG), and industry partners (Google, Cisco, Netflix, etc.) [9, 43, 51]. To continue the development of the latest video coding standards, the reference software algorithms are made publicly available. As open-source software for video compression is directly integrated into research and commercial products. The proposed video compression methods are also accompanied by several detailed specification documents [38] that are regularly published to ensure ease of use by clients. Thus, we assume a white-box model for our attacks, i.e., the adversary knows the DNN-based model used for video compression. We also adopt a white-box model for video classification as explored in prior works [25, 35, 50].

In our offline attack scenario, the adversary can intercept and add perturbations before the victim transmits videos to a cloud server as explained in Section 3.1. Specifically, the adversary can manipulate the systems via malware, or perform man-in-the-middle attack to perturb the raw or compressed videos. To construct our online attack via universal perturbations, we assume the attacker has access to a set of public (benign) videos.

4 Attack Construction

In this section, we explain our three attacks video compression and classification for both online and offline scenarios. We first formulate the attack as an optimization problem to craft the adversarial perturbations. Then, we approximate the QoE function to manipulate the R - D relationship for our proposed attacks. Finally, we construct offline attacks and online universal attacks.

4.1 Attacks as Optimization Problems

Adversarial Attacks on Video Compression. Let $X = \{x_1, x_2, \dots, x_t, \dots, x_T\} \in \mathbb{R}^{T \times W \times H \times C}$ denote an original video clip containing T consecutive frames. Here, x_t represents the frame at a time step t which contains H rows, W columns and C color channels. Let $\Delta = \{\delta_1, \delta_2, \dots, \delta_t, \dots, \delta_T\} \in \mathbb{R}^{T \times W \times H \times C}$ denote a perturbation set for a given video X . We denote an adversarial video by $\bar{X} = \{\bar{x}_1, \bar{x}_2, \dots, \bar{x}_t, \dots, \bar{x}_T\} \in$

$\mathbb{R}^{T \times W \times H \times C}$ and each adversarial frame by $\bar{x}_t = x_t + \delta_t$. Video compression is a function $\mathcal{V}(\bar{x}_t) = \hat{x}_t$ that accepts an adversarial input \bar{x}_t at a time step t and produces an adversarially decoded frame \hat{x}_t using several reference frames stored in the decoded frames’ buffer. Figure 5 demonstrates our attack to the video compression module ($\mathcal{V}(\cdot)$), along with the corresponding inputs, outputs, and the adversarial perturbation.

We define two important factors of back-end subscriber QoE, i.e., bit-rate R and distortion D , as the overall performance metrics of video compression. In other words, these factors refer to end-users’ expectations for frame resolution, which is directly affected by network bandwidth, and video quality. Our set of QoE factors is denoted by $\{Q_0, Q_1\}$, where Q_0 and Q_1 represent expectations for network bandwidth and video quality, respectively. The adversary’s goal is to minimize one QoE factor $Q_p \in \{Q_0, Q_1\}$ while preserving the other Q_{1-p} to ensure stealthiness. We thus formulate our adversarial attacks as the following optimization problem:

$$\begin{aligned} \min_{\Delta} \quad & Q_p(\bar{X}) \\ \text{s. t.} \quad & \begin{cases} \|Q_{1-p}(\bar{X}) - Q_{1-p}(X)\|_2 < \epsilon_q \\ \|X - \bar{X}\|_2 < \epsilon_c \end{cases} \end{aligned} \quad (1)$$

where $Q_p(\bar{X})$ is the expected value of p -th QoE factor for a given adversarial video \bar{X} . $Q_{1-p}(\bar{X})$ is constrained to be the same as the expected value $Q_{1-p}(X)$ for the original video X . To enforce this constraint, we introduce an upper bound ϵ_q on the ℓ_2 norm of the difference. We additionally enforce an upper bound of ϵ_c on the perturbation norm.

Compression-robust Attacks on Video Classification. Figure 5 illustrates a video classification module appended to the video compression pipeline. Video classification relies on a discriminant function $F_c(\hat{X})$ that takes as input a video clip X and outputs a probability distribution over a set K of class labels. $F_c(X)$ indicates the probability of the input video belonging to a specific class $c \in K$. The video classifier $\mathcal{C} : \mathbb{R}^{T \times W \times H \times C} \rightarrow K$ maps an input X to the class with the maximum probability as follows:

$$\mathcal{C}(X) = \arg \max_{c \in K} F_c(X). \quad (2)$$

Let $\hat{X} \in \mathbb{R}^{T \times W \times H \times C}$ be an adversarially decoded video for an original X . The untargeted attack against \mathcal{C} generates perturbations such that $\mathcal{C}(\hat{X}) \neq \mathcal{C}(X)$, whereas the targeted attack aims at $\mathcal{C}(\hat{X}) = c^* (\neq \mathcal{C}(X))$ for a predetermined incorrect class $c^* \in K$. The adversarial loss \mathcal{L}_{adv} for the untargeted and targeted attacks can be written as:

$$\mathcal{L}_{adv} = \begin{cases} F_{\mathcal{C}(X)}(\hat{X}) - \max_{c \neq \mathcal{C}(X)} F_c(\hat{X}) & \text{(Untargeted)} \\ \max_{c \neq c^*} F_c(\hat{X}) - F_{c^*}(\hat{X}) & \text{(Targeted)} \end{cases} \quad (3)$$

Both attacks gain success if and only if $\mathcal{L}_{adv} < 0$. To create versatile perturbations that are robust to compression and capable of QoE attacks, we formulate our attacks against video

classification with consideration for both video compression and classification. Specifically, the adversarial perturbation set Δ is instantiated by minimizing a target QoE factor while satisfying $\mathcal{L}_{adv}(\tilde{X}) < 0$ as follows:

$$\begin{aligned} \min_{\Delta} \quad & Q_p(\tilde{X}) \\ \text{s. t.} \quad & \begin{cases} \|Q_{1-p}(\tilde{X}) - Q_{1-p}(X)\|_2 < \varepsilon_q \\ \mathcal{L}_{adv}(\tilde{X}) < 0 \\ \|X - \tilde{X}\|_2 < \varepsilon_c \end{cases} \end{aligned} \quad (4)$$

4.2 Approximating QoE Factors

Deep learning-based video compression frameworks [31, 55] take advantage of an efficient hybrid coding structure, which mainly comprises spatial and temporal predictions. During the training process, the frames within each GOP are assumed to be independent when performing the R - D optimization. Specifically, the R - D cost is only minimized for the current frame x_t . The victim video compression model is thus built by solving the following R - D optimization:

$$\min_w R_t(x_t) + \lambda \cdot D_t(x_t), \quad (5)$$

where w represents model parameters, and R_t and D_t are the rate and distortion for the t -th frame, respectively. Here, λ is a hyperparameter that controls the trade-off between the number of bits and the distortion.

The R_t and D_t in Equation 5 are insufficient to approximate the QoE factors. This is due to the temporal coding structure within each GOP where the coding of x_t is conditioned upon the coding of its preceding frame. The temporal predictive coding constructs a chain of dependency between all adjacent frames in each GOP. To account for the inter-frame dependency (IFD) throughout a video sequence, our proposed adversary focuses on the average performance of the video coder. We construct our attacks based on the following adversarial R - D model considering the IFD in one GOP:

$$\begin{aligned} \mathcal{L}_{IFD} &= \frac{1}{G} \sum_{t=1}^G (R_t(\tilde{x}_t) + \lambda \cdot D_t(x_t, \tilde{x}_t)) \\ &= \frac{1}{G} \sum_{t=1}^G (H(\tilde{x}_t) + \lambda \cdot d(x_t, \mathcal{V}(\tilde{x}_t))), \end{aligned} \quad (6)$$

where G is the number of frames within each GOP. Here, $H(\tilde{x}_t)$ represents the number of bits used for encoding the latent representations of the perturbed video \tilde{x}_t . Note that $H(\tilde{x}_t)$ directly controls the bitstreams generated by encoding both the motion and residual representations. $d(x_t, \hat{x}_t)$ denotes the distortion between x_t and \hat{x}_t and can be measured using the mean square error (MSE).

Equation 6 can be decomposed into two parts within the same GOP to obtain the expected value of the bit-rate ($H(\cdot)$) and the expected value of distortion ($d(\cdot, \cdot)$). We estimate the

QoE factors for the entire video using the expectations of bit-rate and distortion at intervals of GOP size as follows:

$$Q_p = \begin{cases} \frac{1}{G} \sum_{g=0}^U \sum_{t=1}^G H(\tilde{x}_t) & \text{if } p = 0 \\ \frac{1}{G} \sum_{g=0}^U \sum_{t=1}^G \lambda \cdot d(x_t, \hat{x}_t) & \text{if } p = 1 \end{cases} \quad (7)$$

where U is $\lceil \frac{T}{G} \rceil$ and $\hat{x}_t = \mathcal{V}(\tilde{x}_t)$. Note that here, each x_t within the g -th GOP corresponds to the $(G \cdot g + t)$ -th frame in the entire video sequence. Using the above formulations for Q_p , we generate our adversarial perturbations following the optimization objective in Equation 4.

4.3 Offline Attack Methodology

In the offline attack scenario, injecting the adversarial perturbations is not latency bound. The attacker can therefore use the entire captured video, before creating and adding the adversarial perturbations. To generate the perturbations, the adversary leverages the proposed approximations of QoE to minimize the following adversarial loss function:

$$\begin{aligned} \min_{\Delta} \quad & \mathcal{L}_{comp}(\tilde{X}) = Q_p(\tilde{X}) + \|\mathbf{E}\|_2 \\ \text{s. t.} \quad & \|X - \tilde{X}\|_2 < \varepsilon_c, \end{aligned} \quad (8)$$

where $\|\mathbf{E}\|_2 = \|Q_{1-p}(\tilde{X}) - Q_{1-p}(X)\|_2$. We use the iterative FGSM [23] method to solve Equation 8 as follows:

$$\begin{aligned} \tilde{X}_{n+1} &= \text{clip}_{0,1}(\tilde{X}_n - \frac{\varepsilon_c}{\rho} \text{sign}(\nabla \mathcal{L}_{comp}(\tilde{X}_n))) \\ \tilde{X}_{n+1} &= \text{clip}_{-\varepsilon_c, -\varepsilon_c}(\tilde{X}_{n+1} - \tilde{X}_0) + \tilde{X}_0, \end{aligned} \quad (9)$$

where ρ is the total number of iterations. Here, \tilde{X}_0 is equal to the original (benign) frame X and the final perturbed video \tilde{X} will be equal to \tilde{X}_ρ from the last iteration of Equation 9.

Equation 8 delivers the perturbations for downgrading the performance (QoE) of the video compression system itself. The adversary can optionally choose to repurpose the QoE attack to also affect a downstream video recognition system. In such scenarios, we integrate $\mathcal{L}_{adv}(\tilde{X})$ from Equation 3 to simultaneously derive perturbations on video compression and classification. Therefore, we convert Equation 8 to the following objective function:

$$\begin{aligned} \min_{\Delta} \quad & \mathcal{L}_{comp}(\tilde{X}) + \beta \cdot \mathcal{L}_{adv}(\tilde{X}) \\ \text{s. t.} \quad & \|X - \tilde{X}\|_2 < \varepsilon_c, \end{aligned} \quad (10)$$

where β is the weight to adjust the scale of the two loss functions. We use a similar formulation as Equation 9 to solve the above minimization problem. Specifically, we replace the loss function with $\mathcal{L}_{comp}(\tilde{X}_n) + \beta \cdot \mathcal{L}_{adv}(\tilde{X}_n)$ to generate the perturbations for both compression and classification models.

4.4 Online Attack Methodology

Online adversarial attack is particularly challenging since the adversary cannot predict the next frames in the video stream. Generating new perturbations in real-time, i.e., with the same frequency as the video frames (60 fps) is also infeasible. Additionally, the adversary may not be able to align the image perturbations with the video sequence, which reduces the attack performance due to a boundary effect [25, 52]. We thus propose a novel attack that is universally applicable to live video streams using pre-trained perturbations generated offline. Our universal perturbations are input-agnostic and time-invariant, which is suitable online attacks.

In crafting our universal perturbation, we first aim to address the boundary effect that arises due to the nondeterministic boundaries of the input video clips. If not addressed properly, the boundary effect can potentially degrade the attack performance of the adversarial perturbation. To tackle such an issue, we utilize a temporal transformation function $\Gamma(\cdot)$ for the 3D perturbation with a shifting variable τ [25, 52]. Let us denote a universal adversarial perturbation for a GOP by $\Phi = \{\phi_1, \phi_2, \dots, \phi_G\} \in \mathbb{R}^{G \times W \times H \times C}$ by following the principle that videos are encoded in GOP units. We define a permutation function $\Gamma(\Phi, \tau)$ which produces a cyclic temporal shift of the original perturbation Φ by an offset $\tau \in [0, G-1]$:

$$\begin{aligned}\Gamma(\Phi, \tau) &= \{\phi_{1,\tau}, \phi_{2,\tau}, \dots, \phi_{G,\tau}\} \\ &= \{\phi_{(\tau \bmod G)+1}, \phi_{((1+\tau) \bmod G)+1}, \dots, \phi_{((G-1+\tau) \bmod G)+1}\}.\end{aligned}$$

We denote the adversarial video by $\bar{X} = \{x_1 + \phi_{1,\tau}, \dots, x_T + \phi_{(T \bmod G)+1,\tau} | \forall \tau \in [0, G-1]\} \in \mathbb{R}^{T \times W \times H \times C}$. Note that \bar{X} contains all G possible temporal shift transformations to ensure the generalizability of Φ . The video-agnostic universal perturbation is obtained using our formulations in Equations 8 and 10. Instead of applying the adversarial perturbation to one video clip, we obtain the universal perturbation by averaging the value across all benign videos available to the attacker:

$$\begin{aligned}\min_{\Phi} \mathcal{L}_{uni} &= \sum_{i=1}^N \mathcal{L}_{comp}(\bar{X}^i) + \beta \cdot \mathcal{L}_{adv}(\bar{X}^i) \\ \text{s. t. } \|X - \bar{X}\|_2 &< \epsilon_c,\end{aligned}\tag{11}$$

where N is the total number of videos, and X^i is the i -th video clip in the training set. The adversary can set β to zero to limit the scope of the attack to the compression model only, or a non-zero value to attack a downstream video classification system. In the latter scenario, we consider the case where \mathcal{L}_{adv} is untargeted. We iteratively update Φ with the sign of gradients derived from I-FGSM method as shown in Equation 9.

5 Attack Evaluation

In this section, we first evaluate QoE attacks on the video compression systems to see the vulnerability to our bandwidth and

video quality attacks. We then perform QoE and compression-robust classifier attacks by connecting the video compression and classification modules to form one framework.

5.1 Experimental Setup

QoE Attacks. We use the Vimeo-90K dataset [53] to train the video compression models. This dataset contains 89,800 video clips with 7 frames each, with a resolution of 448×256 . We crop the video sequences into a resolution of 256×256 before training. As our victim video compression module, we consider two state-of-the-art models with different structures, namely, DVC [31] and HLVC [55]. We train the two benign models with different λ values ($\lambda = 256, 512, 1024, 2048$) using the benign loss function in Equation 5.

To validate the performance of our attacks, we use the video sequences in the HEVC datasets [43] including classes B, C, and D. Among them, the HEVC class B is a high resolution (1920×1080) dataset, and the HEVC classes C and D have resolutions of 834×480 and 416×240 , respectively. Following the previous methods [31, 55], we test the HEVC datasets on the first 100 frames and set the GOP size to 10. The video quality is evaluated with peak signal-to-noise ratio (PSNR) and the bit-rate is calculated by bits per pixel (Bpp). To generate the adversarial perturbations for the offline and online scenarios, we use the loss function in Equation 8, and the loss function in Equation 11 with $\beta = 0$. We set ϵ_c to $\frac{10}{255}$, following previous studies [25, 35, 50, 52].

Compression-Robust Classifier Attacks. We use the human action recognition dataset UCF-101 [42] and the hand gesture recognition dataset 20BN-JESTER (Jester) [33] to evaluate our attacks. UCF-101 includes 13320 videos from 101 human action categories (e.g., diving, biking, blow-drying hair, cutting in the kitchen). Jester includes 27 gestures recorded by crowd-sourced workers (e.g., sliding hand left, sliding two fingers left, zooming in with full hand, zooming out with full hand). We consider three state-of-the-art video classification models representing diverse learning methodologies including I3D [8], SlowFast [14], and TPN [54]. We employ the pre-trained models available on MMAction2 [24] open-source repository. To generate the offline and online adversarial perturbations, we set $\beta = 0.1$ and $\epsilon_c = \frac{10}{255}$ [25, 35, 50, 52] in the loss functions expressed in Equations 10 and 11.

Benchmarks. We compare our QoE attacks on video compression models with random perturbations of (1) Gaussian noise: $\epsilon_g \sim \mathcal{N}(0, \sigma^2)$ and $\sigma = 0.01$ and (2) Uniform noise: uniformly sampled noise $\epsilon_u \sim [-\epsilon_c, \epsilon_c]$. As our baseline, we include the traditional video coding methods, H.264 [51], H.265 [43], and show that our attack significantly degrades the DNN-based compression performance to lower than legacy methods. We follow the command line in [31] and use FFmpeg with *default* mode to implement H.264 and H.265.

To validate our compression-robust classifier attacks in video recognition models, we compare the performance with

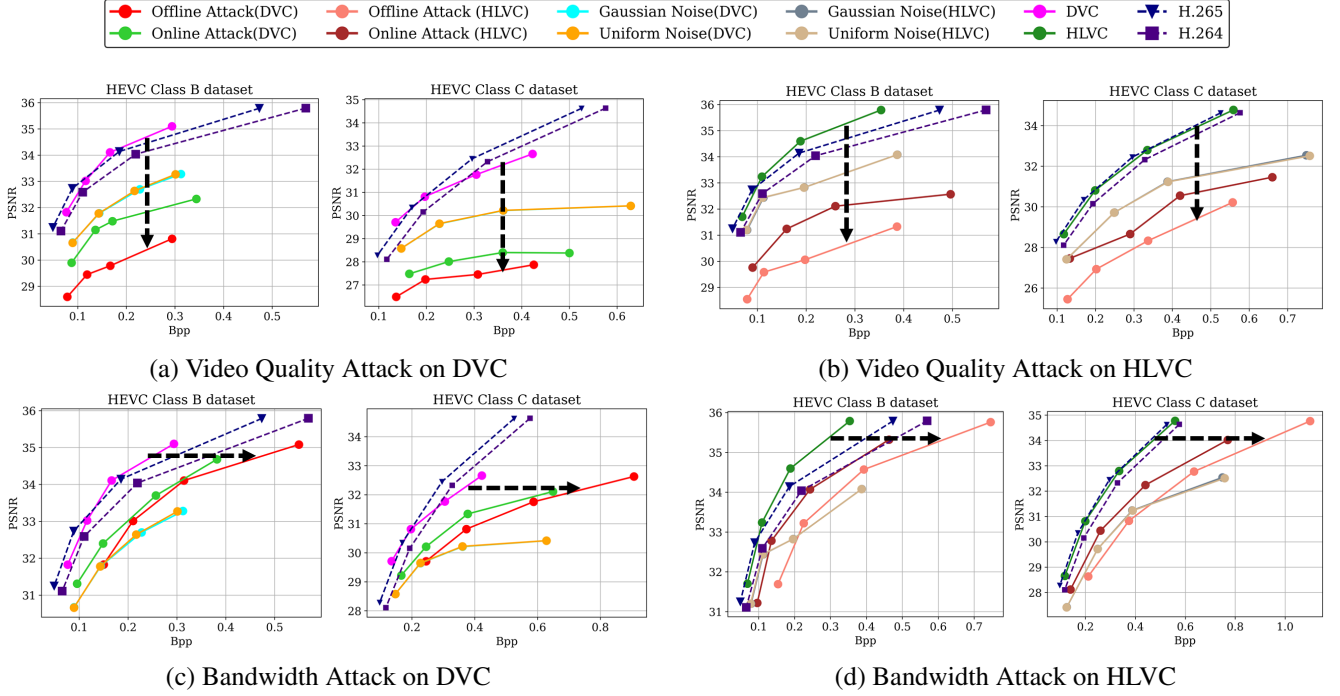


Figure 6: QoE attacks applied to DVC [31] and HLVC [55] video compression frameworks. Each graph contains the results for the victim video compression model trained with $\lambda \in \{256, 512, 1024, 2048\}$.

the following state-of-the-art adversarial attacks on video recognition: Sparse Adversarial Perturbations (SAP) [50], Geometric Transformed Perturbations (GEO-TRAP) [24], and Circular Universal Dual Purpose Perturbation (C-DUP) [25].

5.2 QoE Attacks

In this section, we provide the experimental results to demonstrate the effectiveness of our proposed QoE attacks on benchmarked datasets. We compare our proposed attacks with Gaussian and uniform noise. To enable comparison, we additionally report the benign performance of the victim compression frameworks, namely, DVC [31] and HLVC [55]. Figure 6 demonstrates the PSNR based R - D performance on the HEVC standard test sequences (class B, class C). We report the results for the video quality and the bandwidth attacks in both offline and online settings. Different plots correspond to a video compression model trained with various values, $\lambda \in \{256, 512, 1024, 2048\}$. As λ decreases, the bit-rate of the video compression model improves but the video quality deteriorates. We further report the numerical performance of our QoE attacks in Table 7 in Appendix A.

Figure 8 shows an example of our QoE attacks against DVC on the HEVC dataset. As seen, the performance of the video coder is significantly worse in terms of either PSNR or Bpp, as a result of compressing the perturbed video. Specifically, the benign compressed video and the adversarial video

perturbed with the bandwidth attack show similar image quality after compression although the compression ratio differs by $1.8\times$. We can also see that the video quality attack keeps the Bpp constant but adds several noise-like artifacts to the compressed video that degrade the visual quality.

Analysis of the Video Quality Attack. Figures 6-(a) and (b) show the performance of the proposed video quality attack in the offline and online settings. As seen, our QoE attack can break the R - D model of the pre-trained video encoders (DVC and HLVC) by a large margin. Specifically, our attacks lower the video quality by up to 5.43dB when the λ is 2048 while maintaining the Bpp level. Our attack performance improves when λ is bigger. This is because the bit-rate increases with λ and therefore it is less likely for the perturbations to be removed during compression. Figures 6-(a) and (b) show that video compression is also vulnerable to our universal online attack. Intuitively, the image-agnostic online attack is slightly less powerful than the image-specific offline attack.

The better attack performance of universal perturbations in DVC compared to HLVC can be attributed to the following reasons: 1) HLVC employs the hierarchical temporal coding structures as mentioned in Section 2. By exploiting temporal information from multiple reference frames, the hierarchical structure becomes more error-resistant than non-hierarchical structure. (2) Because of the high correlation among neighboring frames, the low-quality frames can be enhanced using the advantageous information in high-quality frames. This

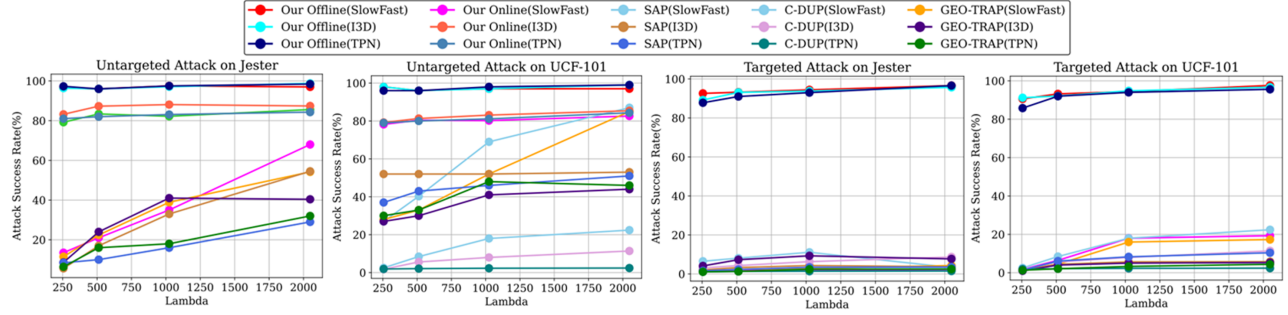


Figure 7: Attack success rate of our compression-robust classifier perturbations compared to prior adversarial attacks on video classification, i.e., SAP [50], GEO-TRAP [24], and C-DUP [25]. We benchmark three video classification models, i.e., I3D [8], SlowFast [14], and TPN [54].

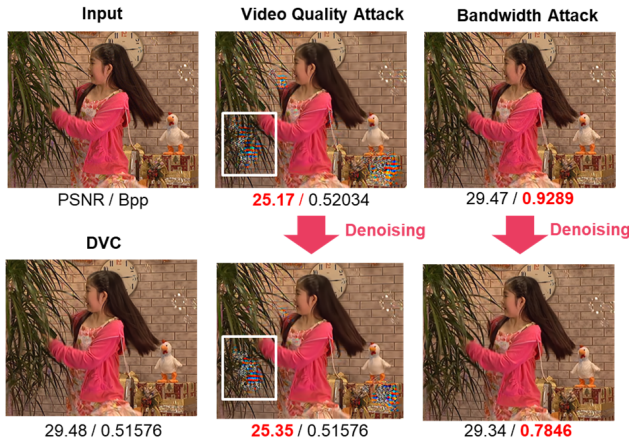


Figure 8: Visual comparison of video compression outputs when the input video is benign versus when the adversary performs QoE attacks on the bandwidth or video quality.

enhancement improves quality without bit-rate overhead, thus improving the rate-distortion performance.

Analysis of the Bandwidth Attack. Figures 6-(c) and (d) demonstrate the performance of our proposed bandwidth attack. As seen, our adversarial perturbations successfully reduce the compression rate of video compression while maintaining the PSNR of the benign models to hide the attack. Gaussian and uniform noise deviate a lot from the R - D curve of the original models and also increase the Bpp level much less than our bandwidth attack. In order to remain stealthy, the perturbed video should not be much different from before. However, Gaussian and Uniform noise differ by at least 0.91dB from the original video quality, which is considerable. When compared with the benign DVC compression model, our proposed bandwidth attack dramatically increases the Bpp level by $\sim 2\times$ on the HEVC class C dataset while reducing the PSNR by only 0.01dB.

5.3 Compression-Robust Classifier Attacks

We compare our proposed attack with the state-of-the-art attacks on video classification, namely, SAP [50], GEO-TRAP [24], and C-DUP [25], and show the vulnerability of existing attacks to video compression. Similar to the threat model for our attacks, we insert the perturbations created by prior work to the inputs of the video compression and classification. The perturbed videos are then compressed and reconstructed by video compression. Finally, they are fed to the victim classifiers. We define the attack success rate as the portion of misclassified test samples for the untargeted attack. For the targeted scenario, the attack success rate is the portion of samples mapped to the adversary’s desired class.

Figure 7 shows the success rate of our bandwidth attack when directed towards a downstream video classifier compared with prior work on adversarial video classification. As seen, our attack achieves the highest success rate. In particular, we obtain over 90% success rate on the UCF-101 and Jester datasets. This is in contrast to prior works, which largely lose their performance once the video is compressed, especially in that targeted scenario.

We visualize some example video snapshots before and after compression in Figure 11 of Appendix B. As observed in Figure 11-(b), the compressed video clips lose some texture information and high-frequency components when compared with the original perturbed video in Figure 11-(a). This effect hinders the attack success rate of prior works. Our well-crafted perturbations, however, can maintain their adversarial effect even when video encoding changes the signal entirely via high-dimensional non-linear transformations. We additionally consider an online attack scenario, where video data is continuously generated and a video clip is classified in real time from the generated video sequence. Even in the complex real-time scenario, our universal perturbations can be injected into both UCF-101 and Jester to achieve a high success rate.

Our proposed attacks not only affect the downstream video classification service but also degrade the performance of the video compression system. In Figure 9 we show the effect of

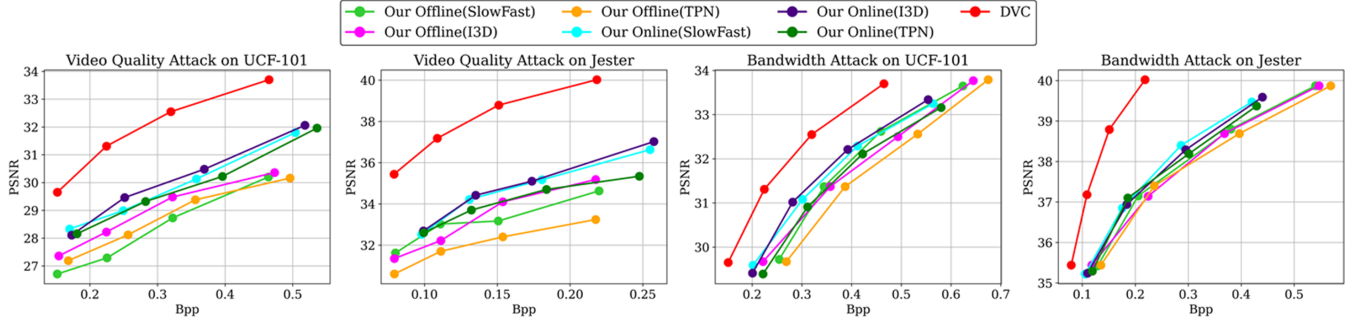


Figure 9: Experimental results of QoE attacks on video compression and classification systems when tested on the UCF-101 and Jester test sets. Each graph contains the results of video compression for the case where $\lambda \in \{256, 512, 1024, 2048\}$.

our attacks for video compression and classification on the PSNR based $R-D$ curve of the DVC compressor module. We observe that our adversarial attacks on video compression and classification can selectively deteriorate the benign compressor’s video quality and bandwidth as explained in Section 5.2. In the example of the Jester dataset, our bandwidth attack increases the Bpp by up to $2.4\times$ while changing the video quality by only 0.1dB. Our video quality attack lowers the PSNR by 4.84dB while changing the Bpp by only 1.47%. Although the online universal attack has lower performance than our offline attack, it lowers the PSNR by up to 3.54dB and increases the Bpp by up to 101.42% on Jester datasets.

We demonstrate the convergence curves of perturbation generation using our losses for targeted and untargeted attacks in Figure 12 of Appendix C. As seen, both losses converge rapidly, and achieve $\sim 100\%$ success rate with 20 FGSM iterations. There is a slight difference in the convergence speed between the bandwidth and the video quality attacks. Since the video quality attack injects the perturbations to greatly downgrade image quality, its overall convergence speed is a bit faster compared to the bandwidth attack.

6 Resiliency to Defense Schemes

In this section, we comprehensively evaluate different defense mechanisms against our adversarial attacks. There are very few defenses available for adversarial video classification. We evaluate the recent defense proposed in [30] which relies on adversarial training (AT). We make slight modifications to the proposed defense method to make it applicable to our attack scenario. In addition, we implement new defense mechanisms that rely on signal transformations to remove adversarial perturbations as shown in Figure 10. For this set of defenses, we are inspired by the literature in image and audio domains [18, 19, 21, 27]. Signal transformation aims at removing the adversarial perturbations from the input video and obtain a clean signal that is similar to the original benign input. We evaluate two signal transformations, namely, JPEG compression [3, 19, 29, 36] and the state-of-the-art video

denoising method [10]. We use the DVC [31] compression model and the HEVC (class C) and UCF-101 datasets for evaluating our attack resiliency against aforesaid defenses.



Figure 10: Overview of the evaluated defenses. The signal transformation aims at reconstructing the original signal while removing the adversarial perturbations.

6.1 Adversarial Training

The performance of AT depends on the adversary’s knowledge regarding the attack algorithms. We assume that the defender has complete white-box knowledge about the perturbations crafted by our attacks. AT expands the training dataset by including all of the adversarial examples generated by the adversary and trains the video compression model on the augmented training dataset. Specifically, the defender adds perturbed videos from every $\lambda \in \{256, 512, 1024, \text{and } 2048\}$ for each QoE attack (bandwidth and video quality) to the clean training dataset. Due to space limitations, we present the results for selected benchmarks in what follows.

Defense against QoE Attacks. As shown in Table 1, the incorporation of adversarial images inside the training comes at a cost of 22.4% higher Bpp and 1.64dB lower PSNR even if the underlying victim model is not attacked. Moreover, the adversarial training cannot protect the video compression model against the QoE attacks. As an example, for the offline attack in Table 1, the video quality attack to the benign model would drop the PSNR by 3.5dB. This drop is reduced to 2.5dB with the adversarial training. However, due to the original 1.64dB drop of PSNR after adversarial training, the total effect on PSNR is even worse than the no defense scenario. For the bandwidth attack, the Bpp is increased by 99.5% when no defense is present and 88.5% with adversarial training. However,

the original 22.4% increase in Bpp due to adversarial training defeats the purpose of the defense. We include additional variations of the datasets and video compression models evaluated against AT in Appendix D.

Table 1: PSNR and Bpp of adversarially trained (AT) [32] DVC on the HEVC class C Datasets.

Benchmark	w Defense		w/o Defense	
	PSNR (dB)	Bpp	PSNR (dB)	Bpp
DVC [31]	29.60	0.32	31.24	0.27
Video Quality (Offline)	-2.47	+0.5%	-3.52	+0.8%
Video Quality (Online)	-2.45	+17.7%	-3.05	+20.0%
Bandwidth (Offline)	-0.06	+88.5%	-0.01	+99.5%
Bandwidth (Online)	-0.67	+32.2%	-0.39	+35.7%

Defense against Compression-Robust Classifier Attacks.

We now present the defense results against compression-robust classifier attacks for the video compression and classification system. Table 2 shows the classification accuracy of the original classification models along with the AT-trained models. We note that AT degrades the accuracy of the benign model significantly which hinders its applicability. We summarize the attack success rate of our targeted and untargeted perturbations in the presence of AT defense in Table 3 and Table 4, respectively. In both tables, we observe that our proposed attacks still achieve a high attack success rate, despite the defense. This is due to the fundamentally complex problem of training a model that is universally robust to multiple adversarial attacks and can simultaneously classify clean video clips correctly. Based on the obtained results, we conclude that our adversarial attacks against video compression and classification are resilient against AT defense mechanism. We include additional results for our online attacks and the Jester dataset in Appendix D.

Table 2: Accuracy of different classification models on clean video clips from the UCF-101 dataset. We report the clean accuracy before and after applying various defense techniques.

Model	Method	Accuracy (%)	Drop (%)
SlowFast [14]	Original	85.4	-
	AT [32]	76.2	-9.2
	JPEG [49]	80.2	-5.2
	Denosing [10]	77.9	-7.5
TPN [54]	Original	74.3	-
	AT [32]	65.8	-8.5
	JPEG [49]	71.8	-2.5
	Denosing [10]	70.3	-4
I3D [8]	Original	71.7	-
	AT [32]	65.2	-6.5
	JPEG [49]	64.4	-7.4
	Denosing [10]	65.9	-5.8

Table 3: Targeted attack success rate (ASR) on video classification in the presence of various defense techniques. Results are gathered on the UCF-101 dataset.

Model	Defense	ASR (%) w Defense	ASR (%) w/o Defense
SlowFast [14]	AT [32]	68.7	
	JPEG [49]	75.5	93.2
	Denosing [10]	76.9	
TPN [54]	AT [32]	65.3	
	JPEG [49]	74.8	92.0
	Denosing [10]	75.3	
I3D [6]	AT [32]	78.5	
	JPEG [49]	80.1	92.1
	Denosing [10]	81.8	

Table 4: Untargeted Attack success rate (ASR) on video classification in the presence of various defense techniques. Results are gathered on the UCF-101 dataset.

Model	Attack	Defense	ASR (%) w Defense	ASR (%) w/o Defense
SlowFast [14]	Offline	AT [32]	67.4	
		JPEG [49]	72.3	96.1
		Denosing [10]	73.3	
	Online	AT [32]	53.8	
		JPEG [49]	64.6	80.4
		Denosing [10]	64.1	
TPN [54]	Offline	AT [32]	65.7	
		JPEG [49]	70.9	95.8
		Denosing [10]	71.8	
	Online	AT [32]	62.3	
		JPEG [49]	61.2	81.3
		Denosing [10]	63.8	
I3D [6]	Offline	AT [32]	77.9	
		JPEG [49]	80.8	96.3
		Denosing [10]	82.7	
	Online	AT [32]	69.4	
		JPEG [49]	72.2	80.7
		Denosing [10]	68.5	

6.2 JPEG Compression

JPEG [49] is a popular lossy compression that applies discrete cosine transform (DCT) on images with different frequencies. We assume that the defender executes JPEG compression as a preprocessing before performing video compression. To compress a perturbed image, the high (low) frequency DCT coefficients are usually scaled more (less). The coefficients are then rounded to the nearest integers by performing a quantization controlled by compression factor (CF). CF directly controls the trade-off between image quality and compression rate, as such, we perform our evaluations with two different values of CF, i.e., 20 and 40.

Defense Against QoE Attacks. The results of JPEG com-

pression against our QoE attacks are summarized in Table 5. As seen, QoE attacks can bypass the widely used JPEG image compression scheme, even when the compression factor CF is set to a high value of 40. Note that when CF=40 in Table 5, we can observe that the compression performance of the clean video is reduced by 1.8dB. This is because texture containing high-frequency information is also removed after JPEG coding. Similar trends can be observed for our online attacks where the JPEG compression does not prevent the effect of the QoE attacks.

Table 5: PSNR and Bpp of DVC on videos preprocessed by JPEG [49] on the HEVC class C Datasets, where CF means compression factor.

Benchmark	CF	w Defense		w/o Defense	
		PSNR (dB)	Bpp	PSNR (dB)	Bpp
DVC [31]	20	31.14	0.28	31.24	0.27
	40	29.26	0.21		
Video Quality (Offline)	20	-3.35	+0.7%	-3.52	+0.8%
	40	-3.14	+0.6%		
Video Quality (Online)	20	-2.86	+19.1%	-3.05	+19.9%
	40	-2.76	+18.4%		
Bandwidth (Offline)	20	-0.25	+95.4%	-0.01	+99.5%
	40	-0.45	+86.7%		
Bandwidth (Online)	20	-1.45	+34.2%	-0.39	+35.7
	40	-1.76	+31.2%		

Defense against Compression-Robust Classifier Attacks.

To evaluate our compression-robust classifier attacks against JPEG compression, we apply our offline and online attacks on UCF-101 datasets. Table 3 summarizes the attack success rate on video classification when JPEG is used as preprocessing before video compression. We see that JPEG fails to defend against our targeted attacks in most cases. In addition, Table 4 shows that compared to the AT defense against untargeted attacks, the performance of JPEG compression is relatively worse. The main reason is that JPEG compression removes adversarial instances on a frame-by-frame basis but it cannot suppress error propagation using a time-series analysis.

6.3 Video Denoising

Denoising is a fundamental video processing algorithm that removes sensor imperfections. We assume that the defender has a noise removal algorithm in the front-end sources, e.g., cameras, before processing the video compression. We use a state-of-the-art DNN-based blind denoiser (ViDeNN) [10] that does not assume any prior environmental conditions, e.g., color and light. As such, ViDeNN can adapt to the external changes where there is a different distribution for each frame.

Defense against QoE Attacks. As seen in Table 6, the addition of the video denoising pipeline at the front-end sources causes a 1.5dB drop in the PSNR of the benign compression model even when the attack is not present. When our proposed video quality attack is applied in the offline and online set-

tings, the PSNR is dropped by 3.23dB and 2.76dB compared to a 3.5dB and 3.05dB drop when the defense is not present, respectively. It can thus be observed that the video quality attack is largely resilient against denoising. Additionally, our bandwidth attack, particularly in the offline setting, still significantly increases the Bpp after video denoising. It is worth noting that the high computational cost of ViDeNN makes it impractical for real-time defense on video content. We conclude that transforming the input signal through video denoising cannot prevent our QoE attacks. As previously shown in Figure 8, even if the defender denoises the perturbed input, the error is still propagated from the perturbed input to the compressed video.

Table 6: PSNR and Bpp of DVC on videos preprocessed by DNN-based denoiser [10] on the HEVC class C Datasets.

Benchmark	w Defense		w/o Defense	
	PSNR (dB)	Bpp	PSNR (dB)	Bpp
DVC [31]	29.74	0.28	31.24	0.27
Video Quality (Offline)	-3.23	+0.5%	-3.52	+0.8%
Video Quality (Online)	-2.76	+14.3%	-3.05	+19.9%
Bandwidth (Offline)	-0.12	+64.8%	-0.01	+99.5%
Bandwidth (Online)	-0.43	+21.8%	-0.39	+35.7%

Defense against Compression-Robust Classifier Attacks.

The denoising operation, by nature, is a lossy transformation that reduces the accuracy of the downstream classifier. As shown in Table 2, denoising the benign streaming video can lead to 4 – 7.5% lower classification accuracy even when the input is not adversarial. Tables 3 and 4 report the attack success rate for targeted and untargeted scenarios when the perturbed video is passed through the denoiser. As can be observed, the targeted attack still maintains a high success rate of 75.3 – 81.8% which is 10.3 – 16.7% lower than when no defense is present. On the untargeted attack scenarios, the denoising reduces the attack success rate by 12.2 – 24% but it remains well above 60% which still poses a critical problem for the classification service. Our results demonstrated that denoising the video cannot successfully remove the effect of injected adversarial perturbations.

7 Related Work

DNN-based Video Compression. In the past decades, plenty of handcrafted image and video compression standards were proposed, such as JPEG [49], JPEG 2000 [41], H.264 [51], and H.265 [43]. Most of these methods follow handcrafted algorithms to remove redundancies in both spatial and temporal domains. Recently, DNN-based video compression frameworks have attracted a lot of attention [17, 31, 55]. Especially, the video compression framework in [31] achieves impressive results by replacing all the components in the standard H.264/H.265 video compression codecs with DNNs. Deep

learning based video compression techniques rely on convolutional neural networks (CNNs) for their two main design components: (1) optimal flow network for estimating the temporal motion and (2) auto-encoder style network for compressing the motion and residual data.

Compared to handcrafted video compression standards [43, 51], CNN-based optimal flow networks significantly reduce the redundancies in video motion [31]. Furthermore, the R - D optimization adopted in DNN-based video compression enables higher compression efficiency by directly using the number of bits in the optimization procedure. To estimate the bit rates, context models [4, 5, 28, 34, 47] are learned for the adaptive arithmetic coding method which compress discrete-valued data to bit-rates closely approaching the entropy of the representation. More recently, Yang *et al.* [55] shows that hierarchical GOP structure can make use of the advantageous information from high-quality frames by improving the temporal predictive coding.

DNN-based Video Classification. DNNs are widely adopted in live video analysis services such as video activity recognition for health care [16], video surveillance [44], and self-driving cars [20]. One of the widely used approaches for activity recognition is an inflated three-dimensional (I3D) network [8]. This method builds upon a pre-trained image classification model by inflating the convolutional and pooling kernels with an additional temporal dimension. Doing so enables the proposed spatiotemporal convolutions to treat spatial structures and temporal events separately, creating a two-stream approach. Slowfast [14] also adopts a two-stream approach and improves the accuracy for action detection by digesting the input video at different temporal resolutions. More recently, Yang *et al.* [54] propose a generic feature-level Temporal Pyramid Network (TPN) to model speed variations amid different actions.

Adversarial Attack and Defense on Image Domain. The adversarial attack was first proposed by [46] aiming to fool a victim model with small perturbations. Goodfellow *et al.* [15] developed the fast gradient sign method (FGSM) to calculate the perturbation by following the direction of gradients. Kurakin *et al.* [23] extended FGSM to an iterative approach, called iterative FGSM (I-FGSM), and showed higher attack success rates. Recently, adversarial attacks using image compression [12] have been proposed that drop critical information from images. This method optimizes over a trainable quantization table by minimizing the adversarial loss.

In response to adversarial attacks, many prior works suggest adversarial training to improve the robustness of the victim DNN [13, 32, 39, 48]. Nevertheless, adversarial training is known to negatively affect the accuracy on clean samples, thus leading to the much-debated trade-off between accuracy and robustness. Recently, compression-based defense algorithms [3, 19, 29, 36] have been proposed which use lossy compression techniques such as JPEG coding to remove the adversarial perturbations. In the video domain, research on

defenses against adversarial attacks using video compression is not explored in prior methods.

Adversarial Attack and Defense on Video Domain. There are only a few studies that propose adversarial attack on video action recognition models. Wei *et al.* [50] propose an optimization-based method to generate adversarial perturbation for the CNN+RNN video classifier [11]. Pony *et al.* [35] present a flickering attack that changes the color of each frame to obtain an adversarial effect and fool the video recognition model. Li *et al.* [24] employ standard geometric transformations for query-efficient black-box attacks. The attacks proposed in [24, 35, 50] are all performed offline. In this context, the video is decomposed into frames which then undergo adversarial attacks, similar to the image domain.

Li *et al.* [25] train a universal perturbation generator offline and use it to attack real-time video classification systems. The most recent study [52] generates universal 3-dimensional perturbations to subvert real-time video classification systems using a surrogate DNN model. The proposed perturbations in the above studies [24, 25, 35, 50, 52] lose effect once the video is passed through the compression pipeline. As such, they cannot be applied in real-world live video streaming and classification scenarios where video compression is a crucial step, as shown in Figure 1. The proposed attacks on video classification in this work, however, can withstand several lossy signal transformations, e.g., compression and denoising.

There are very few defenses that protect against adversarial attacks on videos [30]. Lo *et al.* [30] perform adversarial training with multiple independent batch normalization layers to learn different perturbation types. In this paper, we show that our attacks are robust to the proposed adversarial training.

8 Conclusion

This paper presents the first systematic study on adversarial attacks to deep learning based video compression systems. We proposed the first attacks that manipulate the Rate-Distortion (R - D) relationship of the video compression model for influencing the user quality of experience (QoE). Our attacks are formalized as well-defined optimization problems, thus resulting in a dramatic degradation of video quality and bandwidth. We also proposed novel targeted and untargeted attacks against a downstream deep learning based video classification system. While the video compression framework inherently invalidates most adversarial examples, our attack is robust to compression. Our comprehensive experiments show that our classification attack outperforms previously proposed attacks in both offline and online settings. Furthermore, our attacks still maintain high attack performance in the presence of various defenses, such as adversarial training, video denoising, and JPEG coding. As a future work, we would like to expand factors affecting the QoE of video compression and classification systems. Establishing effective defense strategies against

our attacks is also a crucial and promising direction.

References

- [1] Twitch official website. <https://www.twitch.tv>.
- [2] Youtube live streaming. <https://www.youtube.com/live>.
- [3] Ayse Elvan Aydemir, Alptekin Temizel, and Tugba Taskaya Temizel. The effects of jpeg and jpeg2000 compression on attacks using adversarial examples. *CoRR*, abs/1803.10418, 2018.
- [4] Johannes Ballé, David Minnen, Saurabh Singh, Sung Jin Hwang, and Nic Johnston. Variational image compression with a scale hyperprior. In *International Conference on Learning Representations (ICLR)*, 2018.
- [5] Johannes Ballé, Valero Laparra, and Eero P. Simoncelli. End-to-end optimized image compression. In *International Conference on Learning Representations (ICLR)*, 2017.
- [6] Nicholas Carlini and David Wagner. Adversarial examples are not easily detected: Bypassing ten detection methods. In *Proceedings of the 10th ACM workshop on artificial intelligence and security*, pages 3–14, 2017.
- [7] Nicholas Carlini and David Wagner. Audio adversarial examples: Targeted attacks on speech-to-text. In *2018 IEEE Security and Privacy Workshops (SPW)*, pages 1–7, 2018.
- [8] Joao Carreira and Andrew Zisserman. Quo vadis, action recognition? a new model and the kinetics dataset. In *Proceedings of the IEEE Conference on Computer Vision and Pattern Recognition (CVPR)*, July 2017.
- [9] Yue Chen, Debargha Murherjee, Jingning Han, Adrian Grange, Yaowu Xu, Zoe Liu, Sarah Parker, Cheng Chen, Hui Su, Urvang Joshi, Ching-Han Chiang, Yunqing Wang, Paul Wilkins, Jim Bankoski, Luc Trudeau, Nathan Egge, Jean-Marc Valin, Thomas Davies, Steinar Midtskogen, Andrey Norkin, and Peter de Rivaz. An overview of core coding tools in the av1 video codec. In *2018 Picture Coding Symposium (PCS)*, pages 41–45, 2018.
- [10] Michele Claus and Jan van Gemert. Videnn: Deep blind video denoising. In *Proceedings of the IEEE/CVF Conference on Computer Vision and Pattern Recognition Workshops*, pages 0–0, 2019.
- [11] Jeffrey Donahue, Lisa Anne Hendricks, Sergio Guadarrama, Marcus Rohrbach, Subhashini Venugopalan, Kate Saenko, and Trevor Darrell. Long-term recurrent convolutional networks for visual recognition and description. In *Proceedings of the IEEE Conference on Computer Vision and Pattern Recognition (CVPR)*, June 2015.
- [12] Ranjie Duan, Yuefeng Chen, Dantong Niu, Yun Yang, A Kai Qin, and Yuan He. Advdrop: Adversarial attack to dnns by dropping information. In *Proceedings of the IEEE/CVF International Conference on Computer Vision*, pages 7506–7515, 2021.
- [13] Hugo Jair Escalante, Manuel Montes, and Luis Enrique Sucar. Particle swarm model selection. *Journal of Machine Learning Research*, 10(2), 2009.
- [14] Christoph Feichtenhofer, Haoqi Fan, Jitendra Malik, and Kaiming He. Slowfast networks for video recognition. In *Proceedings of the IEEE/CVF International Conference on Computer Vision (ICCV)*, October 2019.
- [15] Ian J Goodfellow, Jonathon Shlens, and Christian Szegedy. Explaining and harnessing adversarial examples. *arXiv preprint arXiv:1412.6572*, 2014.
- [16] M. Shamim Hossain. Patient state recognition system for healthcare using speech and facial expressions. *Journal of medical systems* 40, pages 1–8, 2016.
- [17] Zhihao Hu, Guo Lu, and Dong Xu. Fvc: A new framework towards deep video compression in feature space. In *Proceedings of the IEEE/CVF Conference on Computer Vision and Pattern Recognition (CVPR)*, pages 1502–1511, June 2021.
- [18] Shehzeen Hussain, Paarth Neekhara, Shlomo Dubnov, Julian McAuley, and Farinaz Koushanfar. Waveguard: Understanding and mitigating audio adversarial examples. In *30th {USENIX} Security Symposium ({USENIX} Security 21)*, 2021.
- [19] Xiaojun Jia, Xingxing Wei, Xiaochun Cao, and Hassan Foroosh. Comdefend: An efficient image compression model to defend adversarial examples. In *Proceedings of the IEEE/CVF Conference on Computer Vision and Pattern Recognition (CVPR)*, June 2019.
- [20] Hirokatsu Kataoka, Yutaka Satoh, Yoshimitsu Aoki, Shoko Oikawa, and Yasuhiro Matsui. Temporal and fine-grained pedestrian action recognition on driving recorder database. *Sensors*, 18(2):627, 2018.
- [21] Faiq Khalid, Hassan Ali, Hammad Tariq, Muhammad Abdullah Hanif, Semeen Rehman, Rehan Ahmed, and Muhammad Shafique. Qusecnets: Quantization-based defense mechanism for securing deep neural network against adversarial attacks. In *2019 IEEE 25th International Symposium on On-Line Testing and Robust System Design (IOLTS)*, pages 182–187. IEEE, 2019.

- [22] Jaehong Kim, Youngmok Jung, Hyunho Yeo, Juncheol Ye, and Dongsu Han. Neural-enhanced live streaming: Improving live video ingest via online learning. In *Proceedings of the Annual Conference of the ACM Special Interest Group on Data Communication on the Applications, Technologies, Architectures, and Protocols for Computer Communication*, SIGCOMM '20, page 107–125, New York, NY, USA, 2020. Association for Computing Machinery.
- [23] Alexey Kurakin, Ian Goodfellow, Samy Bengio, et al. Adversarial examples in the physical world, 2016.
- [24] Shasha Li, Abhishek Aich, Shitong Zhu, Salman Asif, Chengyu Song, Amit Roy-Chowdhury, and Srikanth Krishnamurthy. Adversarial attacks on black box video classifiers: Leveraging the power of geometric transformations. *Advances in Neural Information Processing Systems*, 34, 2021.
- [25] Shasha Li, Ajaya Neupane, Sujoy Paul, Chengyu Song, Srikanth V. Krishnamurthy, Amit K. Roy Chowdhury, and Ananthram Swami. Stealthy adversarial perturbations against real-time video classification systems. In *Proceedings 2019 Network and Distributed System Security Symposium*, 2019.
- [26] Zhuohang Li, Yi Wu, Jian Liu, Yingying Chen, and Bo Yuan. *AdvPulse: Universal, Synchronization-Free, and Targeted Audio Adversarial Attacks via Subsecond Perturbations*, page 1121–1134. ACM, 2020.
- [27] Ji Lin, Chuang Gan, and Song Han. Defensive quantization: When efficiency meets robustness. *arXiv preprint arXiv:1904.08444*, 2019.
- [28] Jiaheng Liu, Guo Lu, Zhihao Hu, and Dong Xu. A unified end-to-end framework for efficient deep image compression. *CoRR*, abs/2002.03370, 2020.
- [29] Zihao Liu, Qi Liu, Tao Liu, Nuo Xu, Xue Lin, Yanzhi Wang, and Wujie Wen. Feature distillation: Dnn-oriented jpeg compression against adversarial examples. In *2019 IEEE/CVF Conference on Computer Vision and Pattern Recognition (CVPR)*, pages 860–868, 2019.
- [30] Shao-Yuan Lo and Vishal M Patel. Defending against multiple and unforeseen adversarial videos. *arXiv preprint arXiv:2009.05244*, 2020.
- [31] Guo Lu, Wanli Ouyang, Dong Xu, Xiaoyun Zhang, Chunlei Cai, and Zhiyong Gao. Dvc: An end-to-end deep video compression framework. In *Proceedings of the IEEE/CVF Conference on Computer Vision and Pattern Recognition (CVPR)*, June 2019.
- [32] Aleksander Madry, Aleksandar Makelov, Ludwig Schmidt, Dimitris Tsipras, and Adrian Vladu. Towards deep learning models resistant to adversarial attacks. *arXiv preprint arXiv:1706.06083*, 2017.
- [33] Joanna Materzynska, Guillaume Berger, Ingo Bax, and Roland Memisevic. The jester dataset: A large-scale video dataset of human gestures. In *Proceedings of the IEEE/CVF International Conference on Computer Vision Workshops*, pages 0–0, 2019.
- [34] Fabian Mentzer, Eirikur Agustsson, Michael Tschannen, Radu Timofte, and Luc Van Gool. Conditional probability models for deep image compression. In *Proceedings of the IEEE Conference on Computer Vision and Pattern Recognition (CVPR)*, June 2018.
- [35] Roi Pony, Itay Naeh, and Shie Mannor. Over-the-air adversarial flickering attacks against video recognition networks. In *Proceedings of the IEEE/CVF Conference on Computer Vision and Pattern Recognition (CVPR)*, pages 515–524, June 2021.
- [36] Aaditya Prakash, Nick Moran, Solomon Garber, Antonella DiLillo, and James Storer. Protecting jpeg images against adversarial attacks. In *2018 Data Compression Conference*, pages 137–146, 2018.
- [37] Anurag Ranjan and Michael J. Black. Optical flow estimation using a spatial pyramid network. In *Proceedings of the IEEE Conference on Computer Vision and Pattern Recognition (CVPR)*, July 2017.
- [38] Jarosław Samelak, Jakub Stankowski, and Marek Domański. Joint collaborative team on video coding (jctvc) of itu-t sg 16 wp 3 and iso/iec jtc 1/sc 29/wg 11 26th meeting: Geneva, ch, 12–20 january 2017.
- [39] Ali Shafahi, Mahyar Najibi, Amin Ghiasi, Zheng Xu, John Dickerson, Christoph Studer, Larry S Davis, Gavin Taylor, and Tom Goldstein. Adversarial training for free! *arXiv preprint arXiv:1904.12843*, 2019.
- [40] Mahmood Sharif, Sruti Bhagavatula, Lujo Bauer, and Michael K Reiter. Accessorize to a crime: Real and stealthy attacks on state-of-the-art face recognition. In *Proceedings of the 2016 acm sigsac conference on computer and communications security*, pages 1528–1540, 2016.
- [41] A. Skodras, C. Christopoulos, and T. Ebrahimi. The jpeg 2000 still image compression standard. *IEEE Signal Processing Magazine*, 18(5):36–58, 2001.
- [42] Khurram Soomro, Amir Roshan Zamir, and Mubarak Shah. Ucf101: A dataset of 101 human actions classes from videos in the wild. *arXiv preprint arXiv:1212.0402*, 2012.

- [43] Gary J Sullivan, Jens-Rainer Ohm, Woo-Jin Han, and Thomas Wiegand. Overview of the high efficiency video coding (hevc) standard. *IEEE Transactions on circuits and systems for video technology*, 22(12):1649–1668, 2012.
- [44] Waqas Sultani, Chen Chen, and Mubarak Shah. Real-world anomaly detection in surveillance videos. In *Proceedings of the IEEE conference on computer vision and pattern recognition*, pages 6479–6488, 2018.
- [45] Cisco Systems. Cisco visual networking index: Forecast and methodology. 2010.
- [46] Christian Szegedy, Wojciech Zaremba, Ilya Sutskever, Joan Bruna, Dumitru Erhan, Ian Goodfellow, and Rob Fergus. Intriguing properties of neural networks. *arXiv preprint arXiv:1312.6199*, 2013.
- [47] George Toderici, Damien Vincent, Nick Johnston, Sung Jin Hwang, David Minnen, Joel Shor, and Michele Covell. Full resolution image compression with recurrent neural networks. In *Proceedings of the IEEE Conference on Computer Vision and Pattern Recognition (CVPR)*, July 2017.
- [48] Florian Tramèr, Alexey Kurakin, Nicolas Papernot, Ian Goodfellow, Dan Boneh, and Patrick McDaniel. Ensemble adversarial training: Attacks and defenses. *arXiv preprint arXiv:1705.07204*, 2017.
- [49] G.K. Wallace. The jpeg still picture compression standard. *IEEE Transactions on Consumer Electronics*, 38(1):xviii–xxxiv, 1992.
- [50] Xingxing Wei, Jun Zhu, Sha Yuan, and Hang Su. Sparse adversarial perturbations for videos. In *Proceedings of the AAAI Conference on Artificial Intelligence*, volume 33, pages 8973–8980, 2019.
- [51] Thomas Wiegand, Gary J Sullivan, Gisle Bjontegaard, and Ajay Luthra. Overview of the h. 264/avc video coding standard. *IEEE Transactions on circuits and systems for video technology*, 13(7):560–576, 2003.
- [52] Shangyu Xie, Han Wang, Yu Kong, and Yuan Hong. Universal 3-dimensional perturbations for black-box attacks on video recognition systems. In *2022 IEEE Symposium on Security and Privacy (SP)*, 2022.
- [53] Tianfan Xue, Baian Chen, Jiajun Wu, Donglai Wei, and William T Freeman. Video enhancement with task-oriented flow. *International Journal of Computer Vision*, 127(8):1106–1125, 2019.
- [54] Ceyuan Yang, Yinghao Xu, Jianping Shi, Bo Dai, and Bolei Zhou. Temporal pyramid network for action recognition. In *Proceedings of the IEEE/CVF Conference on*

Computer Vision and Pattern Recognition (CVPR), June 2020.

- [55] Ren Yang, Fabian Mentzer, Luc Van Gool, and Radu Timofte. Learning for video compression with hierarchical quality and recurrent enhancement. In *Proceedings of the IEEE/CVF Conference on Computer Vision and Pattern Recognition (CVPR)*, June 2020.

A Additional Results for QoE Attacks

We provide the results of QoE attacks on the DVC model in Table 7.

Table 7: QoE attacks on the DVC compression model.

Attacks	Dataset	PSNR	Bpp
Video Quality (Offline)	Class B	-3.85dB	+0.9%
	Class C	-3.52dB	+0.78%
	Class D	-3.94dB	+0.75%
Video Quality (Online)	Class B	-2.3dB	+13.61%
	Class C	-3.05dB	+19.99%
	Class D	-2.82dB	+20.37%
Bandwidth (Offline)	Class B	-0.0dB	+87.56%
	Class C	-0.01dB	+99.46%
	Class D	0.0dB	+87.52%
Bandwidth (Online)	Class B	-0.5dB	+35.36%
	Class C	-0.39dB	+35.74%
	Class D	0.18dB	+28.72%
Gaussian	Class B	-0.91dB	14.19%
	Class C	-1.35dB	+31.89%
	Class D	-1.02dB	+27.17%
Uniform	Class B	-0.92dB	14.22%
	Class C	-1.34dB	+31.88%
	Class D	-1.04dB	+27.21%

B Visualization of the Video Compression

Figure 11 demonstrates several example video clips before and after they go through compression.

C Convergence Analysis of the Proposed Attacks

Figure 12 shows the loss convergence when optimizing the objective functions in Section 4.

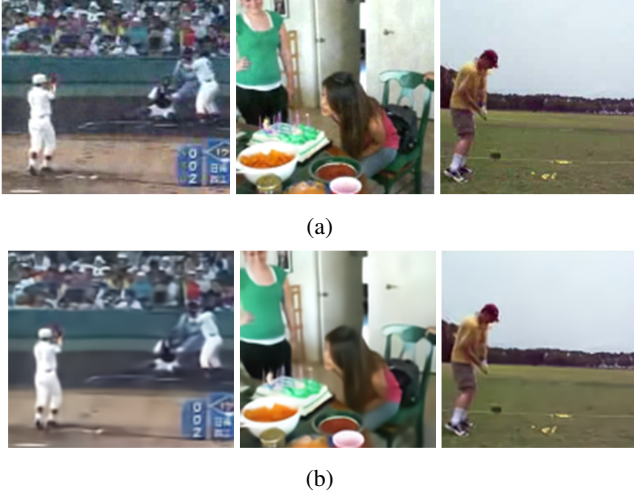


Figure 11: (a) Perturbed video clips versus (b) Compressed video clips. Compressed videos lose some texture information and high frequency components.

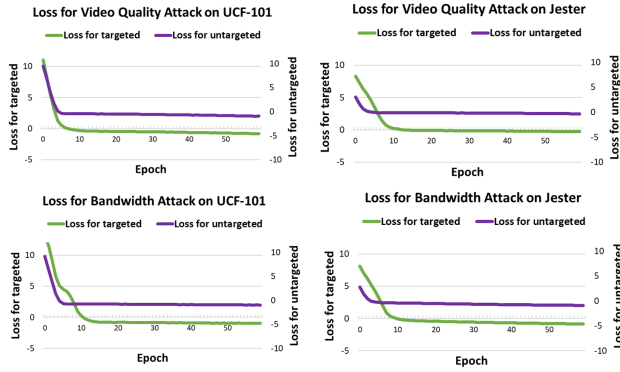


Figure 12: Convergence curves of compression-robust classifier attacks when concurrently performing QoE attacks.

D Additional Results for Resiliency Against Adversarial Training

Table 8, 9, 10, 11, 12, and 13 show the evaluation of robustness of our attacks against adversarial training.

Table 8: PSNR and Bpp of adversarially trained (AT) DVC and HLVC.

Models	Dataset	PSNR	Bpp
Original DVC	Class B	33.52dB	0.1632
	Class C	31.24dB	0.26479
	Class D	31.32dB	0.2796
AT-DVC	Class B	31.39dB	0.1952
	Class C	29.6dB	0.3242
	Class D	29.34dB	0.3302
Original HLVC	Class B	33.83dB	0.18
	Class C	31.36dB	0.3066
	Class D	31.76dB	0.3024
AT-HLVC	Class B	32.46dB	0.2153
	Class C	29.72dB	0.3755
	Class D	30.23dB	0.357

Table 9: Performance difference of adversarially trained DVC.

Attacks	Dataset	PSNR	Bpp
Video Quality (Offline)	Class B	-2.78dB	+0.76%
	Class C	-2.47dB	+0.46%
	Class D	-3.04dB	+0.58%
Video Quality (Online)	Class B	-1.76dB	+14.56%
	Class C	-2.45dB	+17.66%
	Class D	-2.08dB	+18.64%
Bandwidth (Offline)	Class B	-0.07dB	+67.58%
	Class C	-0.06dB	+88.47%
	Class D	-0.03dB	+76.49%
Bandwidth (Online)	Class B	-0.48dB	+31.47%
	Class C	-0.67dB	+32.25%
	Class D	0.37dB	+29.47%

Table 10: Performance difference of adversarially trained HLVC.

Attacks	Dataset	PSNR	Bpp
Video Quality (Offline)	Class B	-2.84dB	+0.57%
	Class C	-2.36dB	+0.39%
	Class D	-2.98dB	+0.74%
Video Quality (Online)	Class B	-2.14dB	+16.98%
	Class C	-3.47dB	+15.47%
	Class D	-1.97dB	+20.33%
Bandwidth (Offline)	Class B	-0.05dB	+64.45%
	Class C	-0.07dB	+79.57%
	Class D	-0.02dB	+73.21%
Bandwidth (Online)	Class B	-0.53dB	+32.55%
	Class C	-0.88dB	+28.98%
	Class D	-0.48dB	+28.45%

Table 11: Accuracy of adversarially trained (AT) video classification models on clean video clips.

Models	Dataset	Accuracy
Original SlowFast	UCF-101	85.4%
	Jester	89.5%
AT-SlowFast	UCF-101	76.2%
	Jester	75.3%
Original TPN	UCF-101	74.3%
	Jester	90.5%
AT-TPN	UCF-101	65.8%
	Jester	81.5%
Original I3D	UCF-101	71.7%
	Jester	91.2%
AT-I3D	UCF-101	65.2%
	Jester	84.1%

Table 12: Targeted attack success rate (ASR) of adversarially trained (AT) video classification models.

Models	Attacks	Dataset	ASR
AT-SlowFast	Offline	UCF-101	68.7%
		Jester	72.4%
AT-TPN	Offline	UCF-101	65.3%
		Jester	71.5%
AT-I3D	Offline	UCF-101	78.5%
		Jester	68.6%

Table 13: Untargeted Attack success rate (ASR) of adversarially trained (AT) video classification models.

Models	Attacks	Dataset	ASR
AT-SlowFast	Offline	UCF-101	67.4%
		Jester	73.4%
	Online	UCF-101	53.8%
		Jester	63.1%
AT-TPN	Offline	UCF-101	65.7%
		Jester	74.3%
	Online	UCF-101	62.3%
		Jester	70.4%
AT-I3D	Offline	UCF-101	77.9%
		Jester	67.2%
	Online	UCF-101	69.4%
		Jester	58.6%